

# First-Principal Calculations of Structural, Electronic and Thermal Properties of ZnGe1-xSnxP2

M. Gasmi<sup>1,2</sup>, S Benlamari<sup>2</sup>, A. Boukortt<sup>1</sup>, A. H. Denawi<sup>3</sup>, S. Meskine<sup>1</sup>, Y. Benkrima<sup>4</sup>

<sup>1</sup>Elaboration and Physical Mechanical and Metallurgical Characterization of Material, Laboratory, ECP3M, Faculty of Sciences and Technology, Abdelhamid Ibn Badis University, Mostaganem, 27000, Algeria.

<sup>2</sup>Laboratoire LPR, Faculté´ des Sciences, Université´ Badji Mokhtar, Annaba, Algeria <sup>3</sup>CNRS, LPICM, École Polytechnique, IP Paris, Palaiseau 91128, France. <sup>4</sup>Ecole Normale superieure de Ouargla, 30000 Ouargla, Algeria Email: mounia.gasmi@yahoo.fr

This paper presents a comprehensive analysis of the structural, electronic, and thermal properties of chalcopyrite compounds ZnGeP2 and ZnSnP2, as well as their mixed crystals ZnGe1-xSnxP2, where x varies from 0 to 1 in increments of 0.25. We used the full-potential linearization augmented plane-wave method (FP-LAPW), incorporating the Wu and Cohen generalized gradient approximation (WC-GGA) for the exchange-correlation potential and Tran and Blaha's modified Becke-Johnson (TB-mBJ) electronic characterization scheme. Ground state properties such as lattice constants, internal parameters, and bulk modulus are computed, demonstrating reasonable agreement with the data available for ZnGeP2 and ZnSnP2. Additionally, the thermodynamic behavior under pressure and temperature effects is examined using the GIBBS program based on the quasi-harmonic model of Debye. Band structure calculations unveil the direct semiconducting band gap nature of ZnGe1-xSnxP2 (x= 0, 1) between the  $(\Gamma-\Gamma)$  symmetry points and the indirect semiconducting band gap nature of ZnGe1-xSnxP2 (x= 0.25, 0.5, 0.75) between them ( $\Gamma$ -M). Alloys of ZnGe1-xSnxP2 with specific compositions are modeled with ordered structures described in periodically repeated supercells.

Keywords: DFT, Alloys, Chalcopyrite, Band Gap, Elastic Constants.

#### 1. Introduction

The ZnGeP2 semiconductor is a promising material with a chalcopyrite structure and a space group of (I.42d). [1] It has high nonlinear optical coefficient (d36 = 75 pm/V) and sufficient birefringence [2], and can be used for frequency doubling, parametric amplification, and other nonlinear processes [3,4]. It can be used as a sensing material for detecting infrared radiation [5,6] and potentially as a material for thin-film solar cells due to its high absorption coefficient and appropriate band gap [7,8]. ZnGeP<sub>2</sub> has a high degree of transparency for wavelength region (0.7–12)µm, and its electronic, elastic, and optical properties have been studied both experimentally and theoretically [9] ZnSnP<sub>2</sub> is another chalcopyrite semiconductor material that has potential applications in various fields. ZnSnP2 has a suitable band gap and high absorption coefficient, making it a promising material for thinfilm solar cells [10,11]. It has potential as a photo catalyst for water splitting and other chemical reactions [12,13]. ZnSnP<sub>2</sub> has a high carrier mobility and can be used for optoelectronic devices such as light-emitting diodes (LEDs) and photodetectors [14,15]. The main advantage is their ability to combine the advantages of thin film technology with the efficiency and stability of traditional crystalline silicon cells. The use of solar cells with chalcopyrite structure in the present and future with solar energy via photovoltaic solar cells is the most direct and efficient method [2, 6]. Photovoltaic materials used for solar cells should possess three significant characteristics: suitable direct gaps, a large absorption coefficient, and high photoelectric conversion efficiency [16, 17]. It is an excellent optical material exhibiting a theoretical photovoltaic conversion efficiency of up to 30% at the Shockley-Queisser limit under AM 1.5G sunlight [18]. Jaffe [19] reported self-consistent full electron density functional calculations of the electronic structures of five chalcopyritestructured semiconductors (ZnSiP<sub>2</sub>, ZnGeP<sub>2</sub>, ZnSnP<sub>2</sub>, ZnSiAs<sub>2</sub>, and MgSiP<sub>2</sub>), and also determined their energy band structures, bonding modes, and charge distributed, Sahin [20] studied the structural, elastic, electronic, and optical properties of ZnSnP2 using a firstprinciples approach of plane-wave pseudo potentials under the local density approximation. ZnSnP<sub>2</sub> has a low thermal conductivity and high Seebeck coefficient, making it a potential material for thermoelectric applications [21,22]. Overall, ZnGeP<sub>2</sub> and ZnSnP<sub>2</sub> have shown great potential and promising materials for various applications and continue to be an active area of research to advance. It is well known that doping crystals with atoms leads to changes in lattice symmetry and diversification in chemical composition, ultimately resulting in a wide variety of crystal properties. To fill this gap, we also analyze how substituting the Ge atoms with Sn ones could modify the structural, electronic, and thermodynamic properties of  $ZnGe_{1-x}Sn_xP_2$  (x = 0, 0.25, 0.5, 0.75, 1). To the best of our knowledge, no experimental or theoretical investigations of the ZnGe<sub>1-x</sub>Sn<sub>x</sub>P<sub>2</sub> alloys have appeared in the literature. The paper is organized as follows: Section 2 describes the calculation procedure. The results and their discussions are presented in Section 3. In the last section, we provide a summary of the results and conclude the article.

#### 2. Computational Details

First-principles calculations have been performed within the density functional theory (DFT) [23, 24] via the the full potential linearized augmented plane-wave method (FP-

## LAPW) [25]

"First-principles calculations have been performed using density functional theory (DFT) [23, 24] via the full-potential linearized augmented plane-wave (FP-LAPW) method [25]."

implemented in the Wien2K code [26]. The exchange-correlation interactions are addressed through the application of the Wu and Cohen generalized gradient approximation (WC-GGA) [27], a modified version of the widely used Perdew-Burke-Ernzerhof approximation (PBE-GGA) [28]. To analyze electronic properties, calculations of the electronic band structure are conducted utilizing both the WC-GGA and modified Becke-Johnson (mBJ) approximations [29]. This approach aims to circumvent the issue of energy gap underestimation inherent in the GGA approximation. The FP-LAPW method is employed, which involves dividing space into interstitial regions (IRs) centered on atomic positions and non-overlapping muffin-tin spheres (MTs). Within the infrared range, the basis comprises plane waves. In the case of MTs, the basis set for a sphere is characterized by the radial solution of the single-particle Schrödinger equation at a fixed energy, along with its energy derivative multiplied by spherical harmonics. To achieve convergence of the energy eigenvalues, the charge density and electric potential in the MT sphere are represented by spherical harmonics up to lmax = 10. To develop the wave function in the gap region, a plane wave boundary Kmax = 8 RMT is chosen (RMT is the smallest muffin radius in the unit cell), and the charge density is expanded by Fourier to  $G_{max} = 12(Ryd)^{1/2}$ . A grid of 32 special K-points in the Brillouin zone binding wedge is used for the total energy calculation. Both the plane wave threshold and the number of k-points are varied to ensure full energy convergence.

#### 3. Results and discussions

### 3.1. Structural properties

ZnGe<sub>1-x</sub>Sn<sub>x</sub>P<sub>2</sub> compounds are tetragonal for different values of x. However, their space groups are I-42d (No.122) for x=0 and 1,  $81_p-4$  for x=0.25, x=0.5 and x=0.75, respectively, and  $\alpha=\beta=\gamma=90^{\circ}$  for the both. This Quaternary Compounds have been investigated for semiconductors crystallized in the chalcopyrite structure with interesting structural, electronic and thermal properties. In the study of structural properties of the Quaternary compound  $ZnGe_{1-x}Sn_xP_2$  (x = 0, 0.25, 0.50, 0.75 and 1) in the chalcopyrite crystal structure are calculated using WC-GGA. To calculate the ground state properties of these compounds, the sum of calculates energy for a specific unit cell volume group. Fit the calculated total energy volume data with the Murnaghan equation of state [30] to determine ground state properties such as the lattice constant (a), internal structural parameters (u) and bulk modulus (B). The results for lattice constant and bulk modulus of our and other work are listed and shows in Table I. The investigated compounds are in good agreement with previous data for the compound ZnGeP2 and ZnSnP2, which demonstrates the high accuracy of the performed calculations and the reliability of the obtained results for these optimized crystal structures and no experimental results neither in the literature on our ZnGe<sub>1-x</sub> Sn<sub>x</sub>P<sub>2</sub> alloy (0.25 0.5 and 0.75). Then, our results can serve as a prediction for future investigations. Fig.1 shows the composition dependence of the calculated lattice parameters (a) and (c) for "For  $ZnGe_{1-x}Sn_xP_2$  with different values of x, we also plotted the bulk modulus curve based on the percentage, From this, we conclude that there is a decrease." of bulk modulus when we add percentage of Sn.

Table1: Equilibrium structural properties of  $ZnGe_{1-x}Sn_xP_2$  (x = 0, 0.25, 0.50, 0.75, 1) lattice constant (A°), c/a ratio, distortion parameter u, bulk modulus B (in GPa) and its first derivative with respect to pressure B` obtained using WC-GGA approximation.

| $ZnGe_{1-x}Sn_xP_2$ |           | a (A°)     | c (A°)     | u ( A°)   | B (Gpa)    | В'        |
|---------------------|-----------|------------|------------|-----------|------------|-----------|
|                     | Our Work  | 5.455      | 10.718     | 0.254     | 79.3[36]   |           |
|                     | Exp       | 5.465 [31] | 10.700[31] | 0.265[31] | 73.60[34]  | 3,0[37]   |
| $\mathbf{x} = 0$    |           | 5.463[32]  | 10.740[32] | 0.254[33] | 88.35[34]  |           |
|                     | Other Cal | 5.502[33]  | 10.850[33] | 0.259[35] | 72.50[35]  | 5.34[35]  |
|                     |           | 5.454[34]  | 10.707[34] |           |            |           |
| x = 0.25            | Our Work  | 5.464      | 11.015     | 0.740     | 82.374     | 4.674     |
| x = 0.50            | Our Work  | 5.528      | 11.100     | 0.739     | 80.028     | 4.666     |
| x = 0.75            | Our Work  | 5.577      | 11.248     | 0.738     | 77.72      | 4.686     |
| x = 1               | Our Work  | 5,650      | 11,360     | 0,229     | 74,33[36]  | 4,672[39] |
|                     | Exp       | 5,670[36]  | 11,302[36] | 0,239[36] | 73,67[39]  |           |
|                     |           | 5,670[37], | 11,330[37] | 0,25[39]  | 71,476[38] | 4,186[38] |
|                     | Other Cal | 5,649 [38] | 11,355[38] | 0,260[38] |            |           |

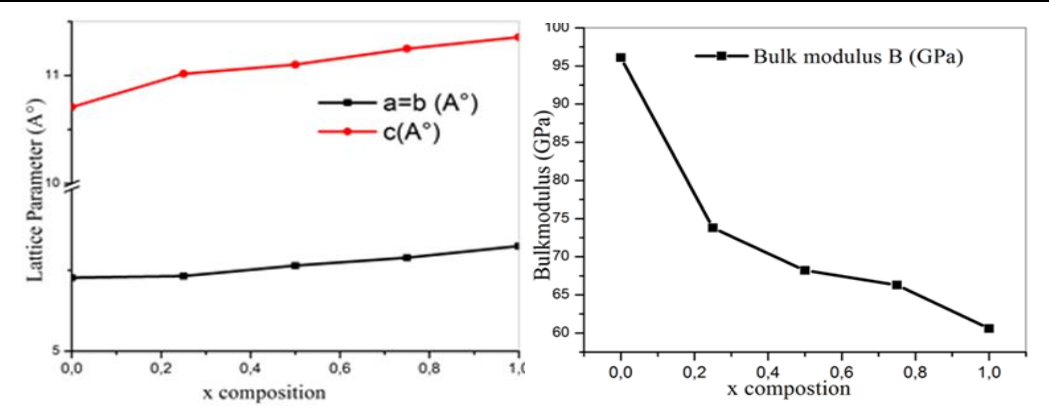


Fig. 1. Composition dependence of the lattice constants and the bulk modulus of Zn  $Ge_{1-x}Sn_xP_2$  (x=0, 0.25, 0.5, 0.75, 1) using WC-GGA.

## 3.2. Electronic properties

In the Quaternary Compounds, we study the electronic properties of  $ZnGe_{1-x}$   $Sn_xP_2$  alloys by calculating the band structure. Calculations are given for the band structures of the considered alloys at concentrations of (0, 0.25, 0.50, 0.75 and 1) Approximate execution using WC-GGA and mBJ. The calculated band gaps are given in Table 2. For these alloys, the band gap is direct  $(\Gamma$ - $\Gamma$ ) for  $ZnGeP_2$  and  $ZnSnP_2$  and indirect  $(\Gamma$ -M) for their mixed  $ZnGe_{1-x}Sn_xP_2$  (x=0.25, 0.5 and 0.75), when Ge atoms are replaced by Sn atoms; the natural band gap does not change. To investigate the behavior of the band gap versus Ge composition x, we track the band gap as a function of concentration using the WC-GGA and mBJ approximations. The results show that the band gap decreases with increasing concentration (Fig.3). The overall profile of the band structure calculated from the two approximations is very similar, except that the band gap values are higher within mBJ, as

Nanotechnology Perceptions Vol. 20 No.4 (2024)

shown in the table 2 along with other first principles and experimental available data.

"It is important to mention that the WC-GGA functional underestimates the energy gap, and this error is attributed to the exchange-correlation energy. In contrast, the modified Becke–Johnson (mBJ) functional provides significantly improved results, which are much closer to the experimental values. High-symmetry directions in the reduced wedge of the Brillouin zone were calculated using the TB-mBJ parameterization schemes for the exchange-correlation potential, as illustrated in Fig. 4."

. There is a good agreement between the present band gap values, obtained using a full potential linear augmented plane wave method, and those previously calculated using other theoretical methods, a good agreement for the band gaps for  $ZnGe_{1-x}Sn_xP_2$  ( x = 0 and x = 01) comparing with the literatures and unfortunately there are no studies yet for x=0.25, 0.50 and 0.75 to compare (see table 2). In fact, when the lattice constant of a semiconductor is increased, it means that the electrons "When the lattice constant increases, the electrons are more loosely bound to the atom, while a decrease in the lattice constant results in the electrons being more tightly bound. In fact, with a larger atomic size, the bond length increases (atomic radius of Sn (1.45 Å) > atomic radius of Ge (1.25 Å) leading to an increase in the lattice constant: a(ZnSnP2) > a(ZnGe<sub>0.25</sub>Sn<sub>0.75</sub>P2) >  $a(ZnGe_0.5Sn_0.5P_2) > a(ZnGe_0.75Sn_0.25P_2) > a(ZnGeP_2)$ . The electrons are more loosely bound to larger atoms, meaning less energy is required to remove them, resulting in a decrease in the band gap: The electrons are loosely bound to the atoms of bigger size and hence require less energy to remove, leading to a decreased band gap Eg (ZnSnP<sub>2</sub>)<Eg (ZnGe<sub>0.25</sub>Sn  $_{0.75}P_2$ ) <.Eg (ZnGe<sub>0.5</sub>Sn  $_{0.5}P_2$ ) <Eg (ZnGe<sub>0.75</sub>Sn  $_{0.25}P_2$ )< Eg (ZnGeP<sub>2</sub>).

Table 2: Band Gap energy of ZnGe<sub>1-x</sub> Sn<sub>x</sub>P<sub>2</sub> alloys for different compositions

|                   | x = 0  |      | x = 0.25   |       | x = 0.50   |       | x = 0.75   |       | x = 1      |                       |
|-------------------|--|------|------------|-------|------------|-------|------------|-------|------------|-----------------------|
| Gap               | WC-<br>GGA                                     | mBJ  | WC-<br>GGA | mBJ   | WC-<br>GGA | mBJ   | WC-<br>GGA | mBJ   | WC-<br>GGA | mBJ                   |
| Our calculation   | 1,20   | 1,90 | 1,124      | 1,914 | 1,112      | 1,899 | 0,998      | 1,766 | 0,20       | 1,20                  |
| Exp               | 1,99[40]                                       |      |            |       |            |       |            |       |            | 2.1[45]               |
| Other calculation | 2,05[41]<br>1,16[42]<br>1,079[43]<br>1,222[44] |      |            |       |            |       |            |       |            | 1.74[46]<br>2.062[47] |

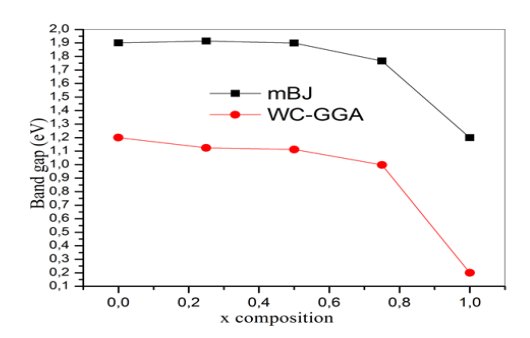


Fig. 2. Composition dependence of the band gap of  $ZnGe_{1-x}Sn_xP_2$  for (x= 0, 0.25, 0.50, 0.75 and 1)

Nanotechnology Perceptions Vol. 20 No.4 (2024)

using both WC-GGA and mBJ.

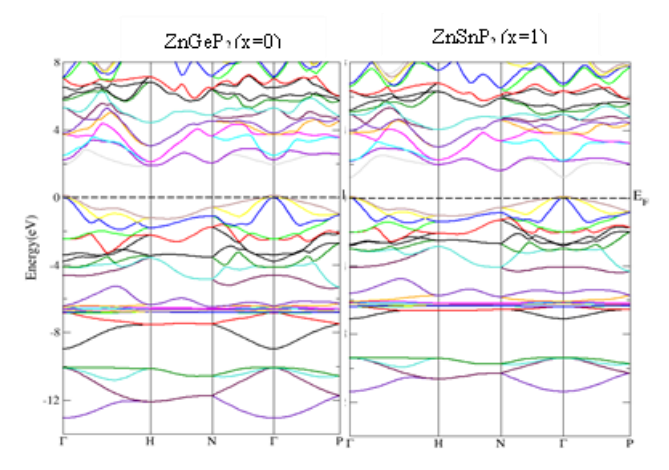


Fig. 3. Calculated band structures of the parent elements of ZnGeP<sub>2</sub> and ZnSnP<sub>2</sub>

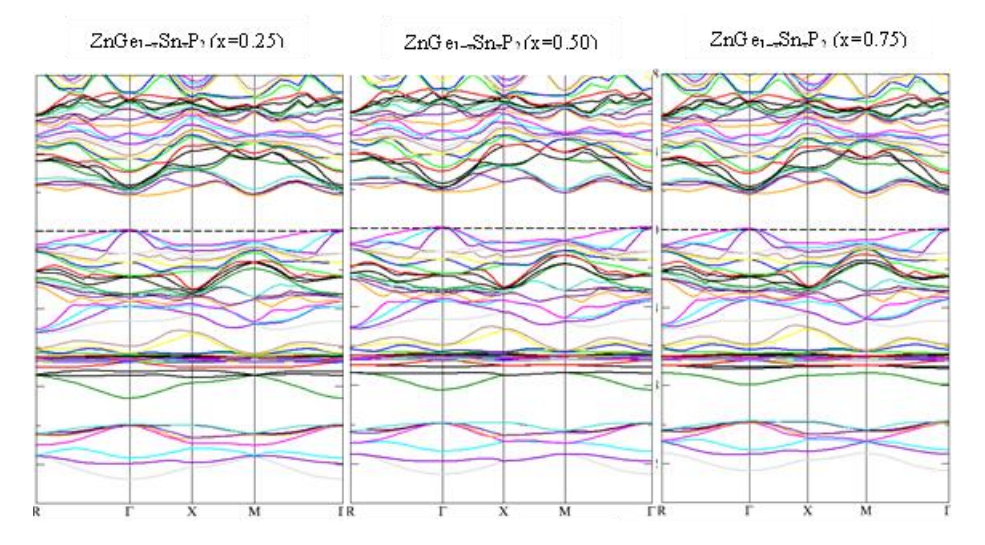


Fig. 4. Calculated band structures of the alloys  $ZnGe_{1-x}Sn_xP_2$  for (x= 0.25, 0.50 and 0.75)

We calculate the total and partial densities of states (TDOS) and (PDOS) for both  $ZnGeP_2$  and  $ZnSnP_2$  and their mixed crystals  $ZnGe_{1-x}Sn_xP_2$  ( $x=0.25,\ 0.5$  and 0.75) to further understand the nature of the band structure and also we have determined the distributions of energy of different electronic states The total DOS (TDOS) and partial DOS (PDOS) are shown in Fig.5 and Fig 6, the DOS obtained only with WC-GGA has been presented. The valence band for all compounds consists of two parts (lower and upper region), as is clearly seen in the total DOS diagram (only the range corresponding to the band structure diagrams is shown). The Fermi level (EF) is taken as an origin of energies. The lower valence band region situated between -11.98 and -10.19 eV, -8.80 and -7.17 eV, and -8.56 and -7.63, eV and -8.22 and -6.94eV and -10.49 and -9.51eV for  $ZnGeP_2$ ,  $ZnGe_{0.75}Sn_{0.25}P_2$ ,  $ZnGe_{0.5}Sn_{0.5}P_2$  and  $ZnGe_{0.25}Sn_{0.75}P_2$  respectively, is essentially dominated by Zn-3d states with a minor contribution of  $ZnGeP_3$  and  $ZnGeP_3$ ,  $ZnGeP_3$ ,

Nanotechnology Perceptions Vol. 20 No.4 (2024)

 $S_{1}$ , Sn-4d and P-3s states (ZnGe<sub>0.75</sub>Sn<sub>0.25</sub>P<sub>2</sub>), and P-3s states (ZnGe<sub>0.5</sub>Sn<sub>0.5</sub>P<sub>2</sub>), and P-3s states and P-3p (,ZnGe<sub>0.25</sub>Sn<sub>0.75</sub>P<sub>2</sub>) and Sn-5s states (ZnSnP<sub>2</sub>). The upper part of the valence band ranging from -9.21 eV to Fermi level (E<sub>F</sub>), -6.92 eV to Fermi level (E<sub>F</sub>), -7.39 eV to Fermi level (E<sub>F</sub>), -6.89 eV to Fermi level(E<sub>F</sub>), -7.45 eV to Fermi level for  $ZnGeP_2$ ,  $ZnGe_{0.75}Sn_{0.25}P_2$ ,  $ZnGe_{0.5}Sn_{0.5}P_2$ ,  $ZnGe_{0.25}Sn_{0.75}P_2$  and  $ZnSnP_2$ , respectively, is mainly due to Ge-4.s and Ge-4p states for (ZnGeP<sub>2</sub>), P-3.s and P-3p states for  $ZnGe_{0.75}Sn_{0.25}P_{2}$  and P-3.s and P-3p states for  $(ZnGe_{0.5}Sn_{0.5}P_{2})$ . P-3s, P-3p states for((,ZnGe<sub>0.25</sub>Sn<sub>0.75</sub>P<sub>2)</sub>, Ge-4.s and Ge-3 p and Ge-3d states for(ZnSnP<sub>2</sub>) with a strong hybridization between the orbitals of each compound. The conduction band consists essentially of Ge-4 s, Ge-4 p, states with a minor presence of P-3 p states for ZnGeP<sub>2</sub>, P-3s, and P-3p states for (ZnGe<sub>0.75</sub>Sn<sub>0.25</sub>P<sub>2</sub>, ZnGe<sub>0.5</sub>Sn<sub>0.5</sub>P<sub>2</sub> and ZnGe<sub>0.25</sub>Sn<sub>0.75</sub>P<sub>2</sub>) and Sn-5p, Sn-5s states with a minor presence of Sn-4d and P-3s states for ZnSnP<sub>2</sub>. Hybridization plays an important role in band gap reduction. In fact, Ge-4.s and Ge-4p states for (ZnGeP<sub>2</sub>), P-3s and P-3p states for (ZnGe<sub>0.75</sub>Sn<sub>0.25</sub>P<sub>2</sub>) and P-3s and P-3p states for (ZnGe<sub>0.5</sub>Sn<sub>0.5</sub>P<sub>2</sub>), P-3s, P-3p states for (ZnGe<sub>0.25</sub>Sn<sub>0.75</sub>P<sub>2</sub>), Ge-4.s and Ge-4 p and Ge-3d states for (ZnSnP<sub>2</sub>which form the upper part of the valence band, repel each other. As a result, the valence band is pushed up, and the band gap is reduced [48].

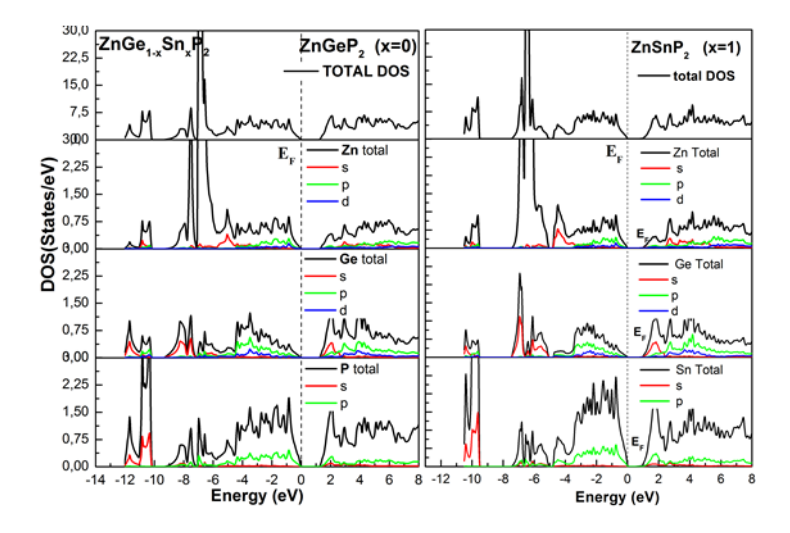


Fig. 5 Total and partial densities of states of the parent elements of ZnGeP<sub>2</sub> and ZnSnP<sub>2</sub>

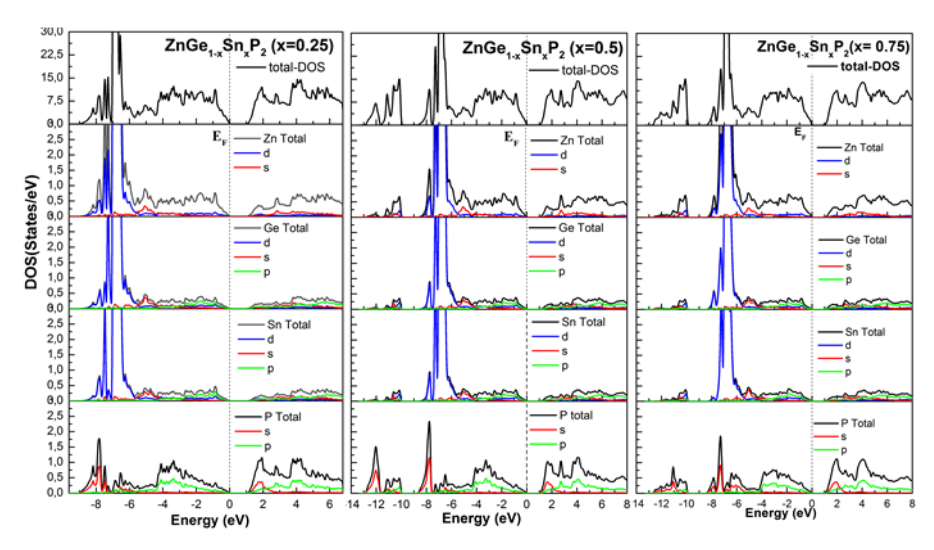


Fig. 6 Total and partial densities of states of  $ZnGe_{1-x}Sn_xP_2$  (x = 0, 0.25, 0.5, 0.75, 1)

# 3.3 Thermal properties

In this section, we present the thermal properties of these materials at various temperatures and pressures. We explore the combined effects of these two external parameters on key thermodynamic properties, including volume (V), bulk modulus (B), Debye temperature ( $\theta$ D), and heat capacities at constant volume ( $C_e$ ). These properties are studied for ZnGeP<sub>2</sub>, ZnSnP<sub>2</sub>, and their mixed compounds ZnGe<sub>1-x</sub>Sn<sub>x</sub>P<sub>2</sub> using the quasi-harmonic Debye approximation, as implemented in the Gibbs calculation program [49]. Research on the properties of materials at high temperature and under stress is crucial for understanding their behavior under extreme conditions. However, measuring very high temperatures at different pressures—specifically at 0, 4, and 8 GPa—can be experimentally challenging or even impossible. In such cases, quantum mechanics, through the use of heat functions, can offer valuable corrections and insights for material behavior.

Researching the properties of materials under high temperatures and stress is essential for understanding their behavior in extreme conditions. However, measuring very high temperatures at various pressures—specifically at 0, 4, and 8 GPa—can be experimentally challenging or even impossible. In such cases, quantum mechanics, particularly through the use of heat functions, can provide valuable corrections and insights into material behavior.

Investigating the thermal properties of materials at high temperatures and under stress is crucial for understanding their behavior under extreme conditions. In addition, sometimes measuring some very high temperatures with three different pressures (0, 4, and 8) GPa will be difficult or Experimentally impossible, but heat function quantum mechanics Then technology also provides important information Regarding the behavior of materials under difficult conditions. In this section, where the input data for the crystal energy E(v) as a function of the volume calculated from first principles used. To study the thermodynamic properties of our alloys, we took a temperature range from 0K to 700K and the pressure range from (0, 4, and 8) GPa. Fig 7 shows the variation of the Bulk modulus B (GPa), for concentrations (x = 0; 0.25; 0.50; 0.75; 1). Note that the Bulk modulus varies inversely with

the temperature it decreases when we increase the temperature for all concentrations, this variation is almost linear, it decreases slightly between 0 and 100 K, then decreases rapidly beyond 100 K.

This variation exhibits a nearly linear trend, with a gradual decrease in the bulk modulus observed between 0 K and 100 K, followed by a more pronounced and rapid decrease at temperatures exceeding 100 K.

It can be seen that, at a given pressure, as the temperature T increases, the bulk modulus results decrease. It is also noted that parent compounds (ZnGeP $_2$  and ZnSnP $_2$ ) are more rigid that their alloys. However, it has been found that the bulk modulus value increases with increasing pressure at a given temperature, Our calculated results of Bulk Modulus (B) at zero temperature and 0 GPa pressure for ZnGe $_{1-x}$ Sn $_x$ P $_2$  (x = 0,0.25,0.5,0.75,1) compounds are 65.5 GPa ,79.8 GPa , 76.5 GPa , 74.5 GPa, and 65.5 GPa respectively.

As we know, the vibration effect is mainly dependent on the temperature, so the calculated characteristics are different Temperature, sensitive to vibration effects.

As is well-known, vibrational effects are primarily temperature-dependent, making the calculated properties highly sensitive to variations in temperature due to these vibrational effects.

The quasi-harmonic Debye model is used to determine thermal properties, where the Debye temperature  $\theta_D$  is the main parameter because it is closely related to many physical properties such as melting point and specific heat. The pressure depends of Debye temperature  $(\theta_D)$  for different concentrations (x = 0, 0.25, 0.50, 0.75 and 1) at several temperatures for the compounds examined is plotted in Fig 8, it can be seen that  $\theta_D$  increases linearly with increasing pressure. However, at a fixed pressure,  $\theta_D$  was found to decrease with increasing temperature. While comparing with bulk modulus it can be seen, most importantly, that the decrease in Debye temperature leads to decreasing compressibility. This is consistent with the fact that  $\theta_D$  is proportional to B, with higher values of  $\theta_D$  providing evidence that the material is stiff. Our calculated results of  $\theta_D$  at temperature (300K) and (0 GPa) pressure for  $ZnGe_{1-x}Sn_xP_2$  (x = 0, 0.25, 0.50, 0.75 and 1) compounds are 387.84 K ,419.56 K , 404.28K , 389.92K, and 336.23K, respectively. Specific heat capacity is an important property of materials, which depends on temperature and vibration characteristics. This property provides necessary insight into many properties, so for many applications, knowledge of it is mandatory. Fig 9 shows the change in heat capacity (C<sub>V</sub> at constant volume) as a function of temperature for our alloy compounds, ZnGe  $_{1-x}Sn_xP_2$  (x = 0, 0.25, 0.50, 0.75 and 1), at different pressures (0, 4 and 8) GPa. The specific heat Cv varies in an almost identical way for all concentrations, it increases rapidly in the range from 0 to 400 K, A rapid increase in heat capacity (Cv) is observed between [0-400] K in all figures for different pressure values[0,4,and 8]GPa and for each concentration., and are proportional to  $T^3$  in the above range. However, for T > 400 K,  $C_V$  tends towards the same limit value for the parent compounds (ZnGeP2 and ZnSnP2) and the same limit value for the compounds alloys, called "Limit of Dulong-Petit. [50] 3.n.R =15R (125.115 J/mol.K), where, n is the number of atoms in the formula unit, R is the universal gas constant. The pressure does not effect on heat capacity results, temperature has a more pronounced effect on heat capacity it depends only on the concentration rate and temperature. The C<sub>V</sub> values obtained at 300 K and 0 GPa for  $ZnGe_{1-x}Sn_xP_2$  (x=0, 0.25, 0.5, 0.75, 1) compounds about 91.90 J.mol-1 K-1for (x=0), 113.32 J.mol-1 K-1 for (x=0.25), 114.08 J.mol-1 K-1 for (x=0.5), 114.78J.mol<sup>-1</sup>K<sup>-1</sup>for (x=0.75), and 93.77J.mol<sup>-1</sup>K<sup>-1</sup>. Fig 10 shows the variation of the volume (V), for the concentrations (x=0, 0.25, 0.50, 0.75 and 1) at (0,4 and 8) GPa and high temperature. Note that the volume varies proportional with the temperature, it increases when we increase the temperature for all concentrations, this variation is almost linear, the pressure does not effect on the volume. Our calculated results of V at zero temperature and 0 GPa pressure

Pressure affects the volume of a material. Our calculated results for volume VVV at zero temperature and 0 GPa pressure:for  $ZnGe_{1-x}Sn_xP_2$  (x=0,0.25,0.50,0.75 and 1) compounds are as follows 562.67 bohr, 561.22 bohr, 578.65 bohr, 596.64 bohr, and 641.69 bohr, respectively. Fig.11 shows the variation of the temperature variation of the coefficient of thermal expansion  $\alpha$ , for different concentrations x, temperature and pressure.

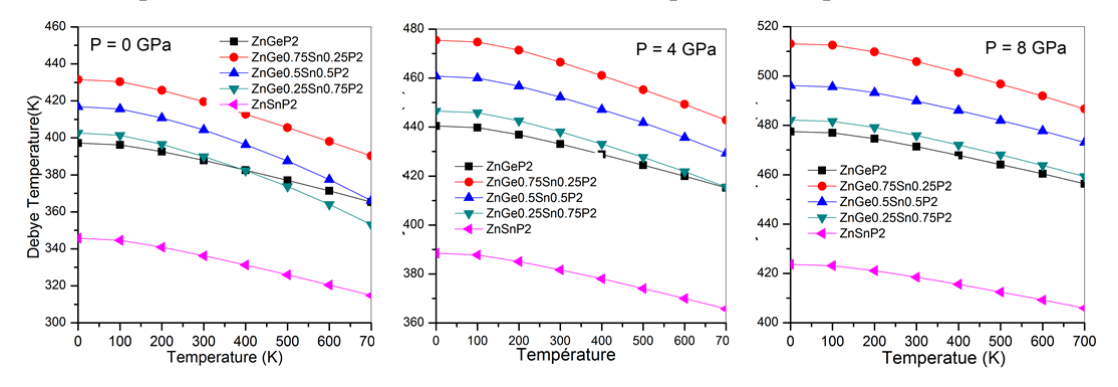


Fig. 8: Variation of Debye temperature as a function of pressure at various temperatures for

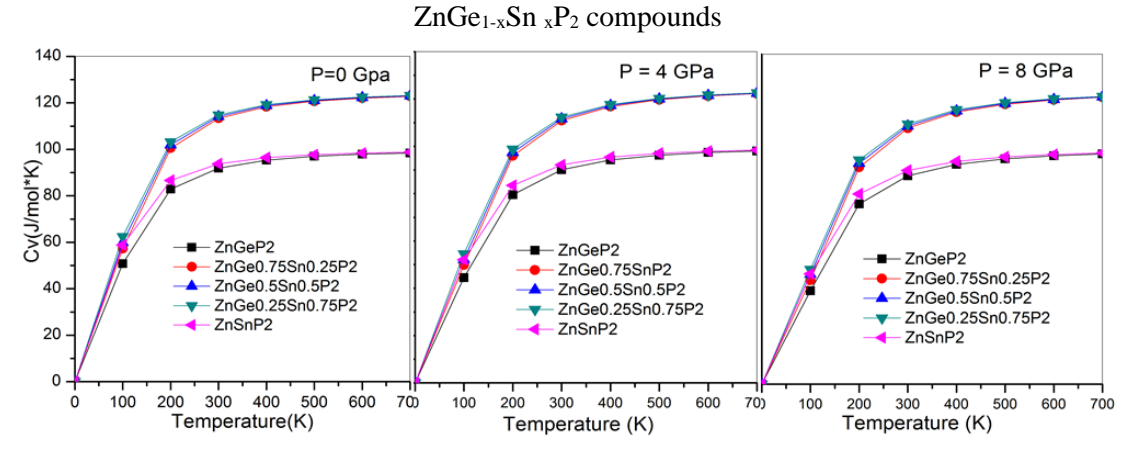


Fig. 9 : Variation of the heat capacities CV versus temperature at various pressures ZnGe<sub>1-x</sub>Sn <sub>x</sub>P<sub>2</sub> compounds

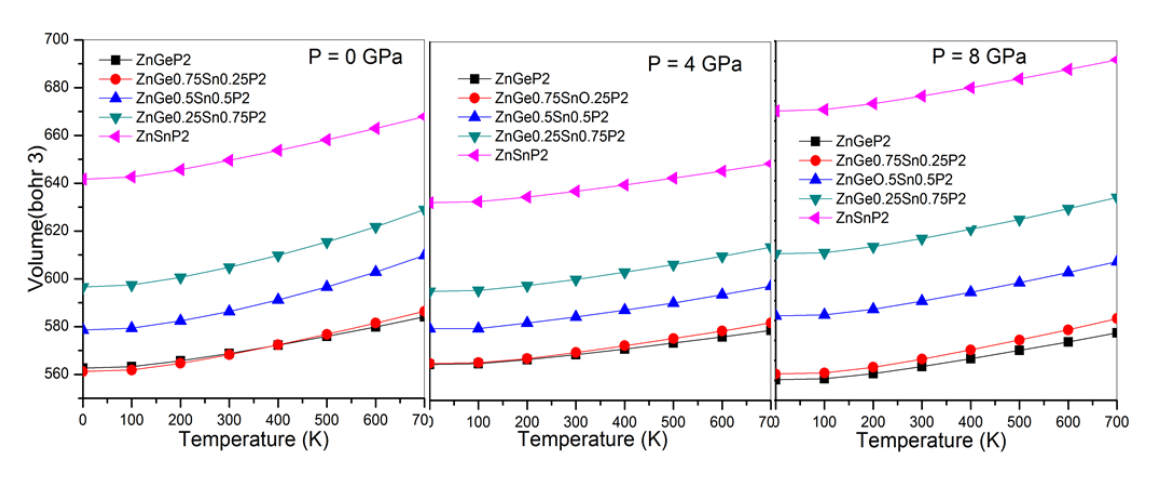


Fig. 10 : Variation of the Volume versus temperature at various pressures for ZnGe <sub>1-x</sub>Sn <sub>x</sub>P<sub>2</sub> compounds

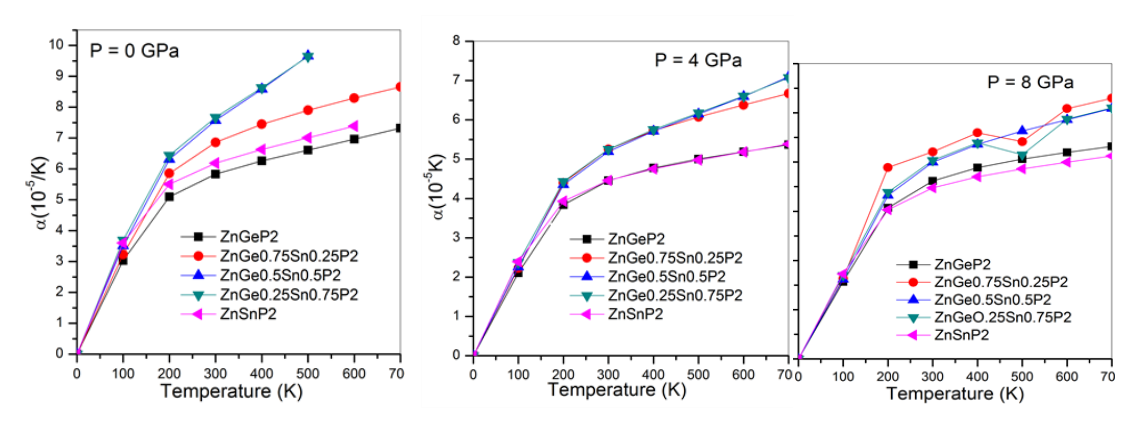


Fig. 11 : Variation of the coefficient of thermal expansion  $\alpha$  as a function of temperature for  $ZnGe_{1-x}Sn_xP_2$  compounds

#### 4. Conclusion

In summary, a comprehensive first-principles investigation was conducted to analyze the structural, electronic, and thermal properties of important chalcopyrite compounds  $ZnGeP_2$ ,  $ZnSnP_2$ , and their mixed crystals  $ZnGe_{1-x}Sn_xP_2$  (x= 0, 0.25, 0.50, 0.75, and 1) across different ambient and pressure conditions. The structural properties, including lattice constants, internal parameters, and bulk modulus, were demonstrated to be highly reliable and in accordance with existing data for the respective compound. These findings were derived from analyses conducted at the WC-GGA level using the FP-LAPW-based WIEN2k approach.

In addition, it was noted that an increase in pressure leads to a reduction in bulk modulus as the unit volume expands. Moreover, the electronic properties of the studied systems were thoroughly investigated using the mBJ exchange-potential. The examination revealed a direct band gap characteristic at  $(\Gamma-\Gamma)$  for the ternary compounds  $ZnGeP_2$  and  $ZnSnP_2$ , whereas an indirect band gap at  $(\Gamma-M)$  was observed for the quaternary  $ZnGe_{1-x}Sn_xP_2$  ( $x=0.25,\ 0.5,\$ and 0.75). Furthermore, there was a linear increase in band gap energy with increasing pressure.

To evaluate the impact of temperature and pressure on the bulk modulus, Debye temperature, and heat capacity, we utilized the quasi-harmonic method of the Debye model and deliberated upon the outcomes. Our findings provide reliable data relevant for potential applications in optoelectronic devices. Notably, no investigation has been conducted on the quaternary  $ZnGe_{1-x}Sn_xP_2$  (x=0.25, 0.50, and 0.75). However, concerning the two ternaries ( $ZnGeP_2$  and  $ZnSnP_2$ ), we observed that the results were in satisfactory agreement.

#### References

- 1. Shay, J. L., & Wernick, J. H. (2013). Ternary chalcopyrite semiconductors: growth, electronic properties, and applications: international series of monographs in the science of the solid state (Vol. 7). Elsevier.
- 2. Ohmer, M. C., & Pandey, R. (1998). Emergence of chalcopyrites as nonlinear optical materials. Mrs Bulletin, 23(7), 16-22.
- 3. Schunemann, P. G., Schepler, K. L., & Budni, P. A. (1998). Nonlinear frequency conversion performance of AgGaSe2, ZnGeP2, and CdGeAs2. Mrs Bulletin, 23(7), 45-49.
- 4. Andreev, Y. M., Geiko, P. P., & Voevodin, V. G. (2000, January). Generator of erbium and CO2 laser combination frequencies. In 13th Symposium and School on High-Resolution Molecular Spectroscopy (Vol. 4063, pp. 246-250). SPIE.
- 5. Bennacer, H., Berrah, S., Boukortt, A., & Ziane, M. I. (2015). Electronic and optical properties of GaInX 2 (X= As, P) from first principles study.
- 6. Lochbaum, A., Dorodnyy, A., Koch, U., Koepfli, S. M., Volk, S., Fedoryshyn, Y., ... & Leuthold, J. (2020). Compact mid-infrared gas sensing enabled by an all-metamaterial design. Nano letters, 20(6), 4169-4176.
- 7. Carnio, B. N., Zawilski, K. T., Schunemann, P. G., Moutanabbir, O., & Elezzabi, A. Y. (2022). The coming age of pnictide and chalcogenide ternary crystals in the terahertz frequency regime. IEEE Transactions on Terahertz Science and Technology, 12(5), 433-445.
- 8. Schnepf, R. R., Tellekamp, M. B., Saenz, T., Mangum, J. S., Supple, E., Roberts, D. M., ... & Tamboli, A. C. (2022). Epitaxial ZnGeP2 thin films on Si and GaP by reactive combinatorial sputtering in phosphine. Crystal Growth & Design, 22(10), 6131-6139.
- 9. Bennacer, H., Boukortt, A., Meskine, S., Hadjab, M., Ziane, M. I., & Zaoui, A. (2018). First principles investigation of optoelectronic properties of ZnXP2 (X= Si, Ge) lattice matched with silicon for tandem solar cells applications using the mBJ exchange potential. Optik, 159, 229-244.
- 10. Gribenyukov, A. (2004). Preparation of ZnGeP2 for nonlinear optical applications: melt and homoepitaxial vapor growth, properties of the grown crystals.
- 11. Tripathy, S. K., & Kumar, V. (2014). Electronic, elastic and optical properties of ZnGeP2 semiconductor under hydrostatic pressures. Materials Science and Engineering: B, 182, 52-58.
- 12. Lee, S., Fahrenkrug, E., & Maldonado, S. (2015). Synthesis of photoactive ZnSnP2 semiconductor nanowires. Journal of Materials Research, 30(14), 2170-2178.
- 13. Nakatsuka, S., Inoue, R., & Nose, Y. (2018). Fabrication of CdSnP2 Thin Films by Phosphidation for Photovoltaic Application. ACS Applied Energy Materials, 1(4), 1635-1640.
- 14. Sheets, E. J. (2015). The solution-based synthesis of semiconducting phosphide nanocrystals

- for alternative energy applications (Doctoral dissertation, Purdue University).
- 15. Oba, F., & Kumagai, Y. (2018). Design and exploration of semiconductors from first principles: A review of recent advances. Applied Physics Express, 11(6), 060101.
- 16. Zhou, X., Gan, L., Zhang, Q., Xiong, X., Li, H., Zhong, Z., ... & Zhai, T. (2016). High performance near-infrared photodetectors based on ultrathin SnS nanobelts grown via physical vapor deposition. Journal of Materials Chemistry C, 4(11), 2111-2116.
- 17. Ramuz, M. P., Vosgueritchian, M., Wei, P., Wang, C., Gao, Y., Wu, Y., ... & Bao, Z. (2012). Evaluation of solution-processable carbon-based electrodes for all-carbon solar cells. ACS nano, 6(11), 10384-10395.
- 18. Shaposhnikov, V. L., Krivosheeva, A. V., Borisenko, V. E., Lazzari, J. L., & d'Avitaya, F. A. (2012). Ab initio modeling of the structural, electronic, and optical properties of A II B IV C 2 V semiconductors. Physical Review B, 85(20), 205201.
- 19. Gautam, R., Singh, P., Sharma, S., Kumari, S., & Verma, A. S. (2015). Structural, electronic, optical, elastic and thermal properties of CdSnP2 with the application in solar cell devices. Superlattices and Microstructures, 100(85), 859-871.
- 20. Shockley, W., & Queisser, H. (2018). Detailed balance limit of efficiency of p-n junction solar cells. In Renewable Energy (pp. Vol2\_35-Vol2\_54). Routledge.
- 21. Jaffe, J. E., & Zunger, A. (1984). Electronic structure of the ternary pnictide semiconductors ZnSiP 2, ZnGeP 2, ZnSnP 2, ZnSiAs 2, and MgSiP 2. Physical Review B, 30(2), 741.
- 22. Sahin, S., Ciftci, Y. O., Colakoglu, K., & Korozlu, N. (2012). First principles studies of elastic, electronic and optical properties of chalcopyrite semiconductor ZnSnP2. Journal of alloys and compounds, 529, 1-7.
- 23. Ramirez, D., Menezes, L. T., & Kleinke, H. (2023). Thermoelectric Properties of the Chalcopyrite Solid Solutions ZnGe1–x Sn x P2. ACS Applied Electronic Materials.
- 24. Guin, S. N., Chatterjee, A., & Biswas, K. (2014). Enhanced thermoelectric performance in ptype AgSbSe 2 by Cd-doping. RSC Advances, 4(23), 11811-11815.
- 25. Hohenberg, P., & Kohn, W. (1964). Inhomogeneous electron gas. Physical review, 136(3B), B864.
- 26. Kohn, W., & Sham, L. J. (1965). Self-consistent equations including exchange and correlation effects. Physical review, 140(4A), A1133.
- 27. Andersen, O. K. (1975). Linear methods in band theory. Physical Review B, 12(8), 3060.
- 28. Blaha, P., Schwarz, K., Madsen, G. K., Kvasnicka, D., & Luitz, J. (2001). wien2k. An augmented plane wave+ local orbitals program for calculating crystal properties, 60(1).
- 29. Wu, Z., & Cohen, R. E. (2006). More accurate generalized gradient approximation for solids. Physical Review B, 73(23), 235116.
- 30. Perdew, J. P., Burke, K., & Ernzerhof, M. (1996). Generalized gradient approximation made simple. Physical review letters, 77(18), 3865.
- 31. Becke, A. D., & Johnson, E. R. (2006). A simple effective potential for exchange. The Journal of chemical physics, 124(22).
- 32. Xiao, H., Tahir-Kheli, J., & Goddard III, W. A. (2011). Accurate band gaps for semiconductors from density functional theory. The Journal of Physical Chemistry Letters, 2(3), 212-217.
- 33. Wohlfarth, C. (2008). 1 Introduction: Data extract from Landolt-Börnstein III/47: Optical Constants. Refractive Indices of Pure Liquids and Binary Liquid Mixtures (Supplement to III/38), 1-2.
- 34. Shaposhnikov, V. L., Krivosheeva, A. V., Borisenko, V. E., Lazzari, J. L., & d'Avitaya, F. A. (2012). Ab initio modeling of the structural, electronic, and optical properties of A II B IV C 2 V semiconductors. Physical Review B, 85(20), 205201.
- 35. Kumar, V., Shrivastava, A. K., & Jha, V. (2010). Bulk modulus and microhardness of tetrahedral semiconductors. Journal of Physics and Chemistry of Solids, 71(11), 1513-1520.
- 36. Vaipolin, A. A., Goryunova, N. A., Kleshchinskii, L. I., Loshakova, G. V., & Osmanov, E. O.

- (1968). The structure and properties of the semiconducting compound ZnSnP2. physica status solidi (b), 29(1), 435-442.
- 37. Scanlon, D. O., & Walsh, A. (2012). Bandgap engineering of ZnSnP2 for high-efficiency solar cells. Applied Physics Letters, 100(25).
- 38. Yuhan Zhong, Huayue Mei, Dafang He, Xue Du, Nanpu Cheng\*, Journal of Physics and Chemistry of Solids 134 (2019) 157–164
- 39. Sahin, S., Ciftci, Y. O., Colakoglu, K., & Korozlu, N. (2012). First principles studies of elastic, electronic and optical properties of chalcopyrite semiconductor ZnSnP2. Journal of alloys and compounds, 529, 1-7.
- 40. Shay, J. L., Tell, B., Buehler, E., & Wernick, J. H. (1973). Band Structure of ZnGe P2 and ZnSiP2—Ternary Compounds with Pseudodirect Energy Gaps. Physical Review Letters, 30(20), 983.
- 41. Jiang, X., & Lambrecht, W. R. (2004). Electronic band structure of ordered vacancy defect chalcopyrite compounds with formula II– III 2– VI 4. Physical review B, 69(3), 035201.
- 42. Rashkeev, S. N., Limpijumnong, S., & Lambrecht, W. R. (1999). Second-harmonic generation and birefringence of some ternary pnictide semiconductors. Physical Review B, 59(4), 2737.
- 43. Chiker, F., Abbar, B., Bresson, S., Khelifa, B., Mathieu, C., & Tadjer, A. (2004). The reflectivity spectra of ZnXP2 (X= Si, Ge, and Sn) compounds. Journal of Solid State Chemistry, 177(11), 3859-3867.
- 44. Tripathy, S. K., & Kumar, V. (2014). Electronic, elastic and optical properties of ZnGeP2 semiconductor under hydrostatic pressures. Materials Science and Engineering: B, 182, 52-58.
- 45. Goodman, C. H. L. (1957). A new group of compounds with diamond type (chalcopyrite) structure. Nature, 179(4564), 828-829.
- 46. Scanlon, D. O., & Walsh, A. (2012). Bandgap engineering of ZnSnP2 for high-efficiency solar cells. Applied Physics Letters, 100(25).
- 47. Zhong, Y., Mei, H., He, D., Du, X., & Cheng, N. (2019). First-principles studies of structural, elastic, electronic, optical and lattice dynamical properties of XSnP2 (X= Zn, Cd and Hg) compounds. Journal of Physics and Chemistry of Solids, 134, 157-164.
- 48. Jaffe, J. E., & Zunger, A. (1984). Theory of the band-gap anomaly in AB C 2 chalcopyrite semiconductors. Physical Review B, 29(4), 1882.
- 49. Blanco, M. A., Francisco, E., & Luana, V. G. I. B. B. S. (2004). GIBBS: isothermal-isobaric thermodynamics of solids from energy curves using a quasi-harmonic Debye model. Computer Physics Communications, 158(1), 57-72.
- 50. Dulong, P. L., & Petit, A. T. (1818). Recherches sur la mesure des températures et sur les lois de la communication de la chaleur. De l'Imprimerie royale.